SAND2018-5818C

ANS RPSD 2018 - 20th Topical Meeting of the Radiation Protection & Shielding Division of ANS
Santa Fe, NM, August 26 – 31, 2018, on CD-ROM, American Nuclear Society, LaGrange Park, IL (2018)

IMPORTANCE OF TREATING CORRELATIONS IN THE UNCERTAINTY QUANTIFICATION OF RADIATION DAMAGE METRICS

Patrick J. Griffin[1], Arjan Konig[2], and Dimitri Rochman[3]

[1]*Sandia National Laboratories, P.O. Box 5800, Albuquerque, NM, USA, 87122, (505) 845-9121, pjgriff@sandia.gov*
[2]*International Atomic Energy Agency, P.O. Box 100 A-1400, Vienna, Austria, (43-1) 2600 21709, a.koning@iaea.org*
[3]*Paul Scherrer Institut, Villigen 5232, Switzerland, (41-56) 310 44 62, Dimitri-alexandre.rochman@psi.ch*

The radiation effects community embraces the importance of quantifying uncertainty in model predictions and the importance of propagating this uncertainty into the integral metrics used to validate models, but they are not always aware of the importance of addressing the energy- and reaction-dependent correlations in the underlying uncertainty contributors. This paper presents a rigorous high-fidelity approach that addresses the correlation in the underlying uncertainty components and quantifies the role of both energy and reaction-dependent correlations in a sample application that addresses the damage metrics relevant to silicon semiconductors.

I. INTRODUCTION

The radiation effects community needs a rigorous high-fidelity quantification of the uncertainty in various damage metrics that are used in the assessment of the radiation response of materials. As a sample application of an approach that should be used, this paper addresses a set of nine damage metrics that are relevant to silicon semiconductors. These metrics are shown in Table I.

TABLE I. Damage metrics relevant to silicon semiconductors.

#	Metric	Units
1	Total dose	rad(Si)
2	Displacement dose	rad(Si)
3	Ionizing dose	rad(Si)
4	1-MeV(Si)-Equivalent Fluence	1-MeV(Si)-Eqv./cm^2
5	NRT damage energy	eV-b
6	Frenkel pair density	FP/μ
7	Track density	Tracks/μ
8	Minority carrier lifetime	μs
9	Cumulative LET distribution	MeV-cm^2/mg

The following sections address: a) the definition of the calculated radiation damage metrics; b) the sources of uncertainty in the calculated metrics; and c) a rigorous quantification of the neutron energy-dependent uncertainty for these damage metrics in the form of a covariance matrices. Complete covariance matrices are given for damage metrics #1, 2, 3, 5, and 7 shown in Table I.

II. DEFINITION OF DAMAGE METRICS

The most fundamental calculated damage metric is the total dose delivered to the sensitive volume of a silicon device. In order to eliminate the sensitivity of this calculated metric to small feature details in the silicon device, for example the presence of metal vias, the assumption is made that charged particle (electron) equilibrium exists. Given this condition, the neutron energy dependence of the total dose is identical to that for the microscopic kerma factor. In order to examine the uncertainty contributors to this damage metric, it is desirable to establish a general framework that can be used to describe the metrics.

Given an energy-dependent microscopic response function, $\Re(E)$, and an incident neutron fluence, $\phi(E)$, the macroscopic observable/metric, D, is given by the expression seen in Equation 1, where £ is a unit conversion that varies with the selected damage metric.

$$D = \int_0^\infty £\, \phi(E)\, \Re(E)\, dE \tag{1}$$

For silicon, when the response function is the microscopic kerma factor as computed within the NJOY-2012 code[1] and reported as the MT=301 quantity in units of eV-b, the unit conversion factor is $3.435\text{x}10^{-13}$ [rad(Si)-cm^2]/[MeV-mb] • $1.\text{x}10^{-3}$ [MeV-mb]/[eV-b].

For a neutron irradiation, the microscopic neutron kerma factor, i.e. $\Re(E) = \kappa_{kerma}(E)$, which is the energy-dependent response used to determine the dose/kerma delivered in the radiation exposure, is computed through the expression shown in Eq. 2.

Sandia National Laboratories is a multi-mission laboratory managed and operated by National Technology and Engineering Solutions of Sandia, LLC, a wholly owned subsidiary of Honeywell International, Inc., for the U.S. Department of Energy's National Nuclear Security Administration under contract DE-NA0003525.

$$ {}^{n}\kappa_{kerma}(E) = \sum_{i,j_i} \sigma_{i,j_i}(E) \int_0^{\infty} dT_{R,j_i} $$

$$ \int_{-1}^{1} d\mu \cdot f(E,\mu,T_{R,j_i}) \cdot T_{R,j_i} \qquad (2) $$

In this expression the summation is over all reaction channels i and all particles, j_i, emitted in that reaction, E is the energy for the incident neutron, $\sigma_{i,j_i}(E)$ is the cross section for producing particle j_i, through reaction i, T_{R,j_i} is the associated recoil particle/ion energy, the integral is over the recoil particle energy and the recoil emission angle, and $f(E,\mu,T_{R,j_i})$ is the energy/angle distribution for the outgoing recoil particle. Conservation of energy and momentum often produce a strong correlation between the outgoing recoil atom energy and its emission angle, which is captured in this term.

The second damage metric in Table I, the microscopic displacement kerma factor is given by:

$$ {}^{n}_{type}\kappa_{displ}(E) = \sum_{i,j_i} \sigma_{i,j_i}(E) \int_0^{\infty} dT_{R,j_i} $$

$$ \int_{-1}^{1} d\mu \cdot f(E,\mu,T_{R,j_i}) \cdot {}^{ion}T_{dam}^{type}\left(T_{R,j_i}\right) \cdot T_{R,j_i} \qquad (3) $$

where ${}^{ion}T_{dam}^{type}\left(T_R\right)$ is the fractional recoil ion damage partition function indicated by the "*type*". Typical "*types*" of the damage partition function used for silicon include: a) the Robinson fit[2] to the Lindhard, Scharff, and Schiott (LSS) energy partition[3]; b) the Akkermann analytic fit[4] based on use of the Ziegler, Biersack, and Littmark (ZBL) potential[5] for the elastic Coulomb scattering and use of a combination of a local (impact parameter dependent) model and a non-local model for the inelastic ion-atom scattering.

The third damage metric, the microscopic ionizing kerma factor is given by:

$$ {}^{n}_{type}\kappa_{ion}(E) = {}^{n}\kappa_{kerma}(E) - {}^{n}_{type}\kappa_{displ}(E) \qquad (4) $$

The fourth damage metric, the ASTM 1-MeV(Si)-Equivalent fluence[6,7], is defined to be equal to the displacement kerma divided by a reference displacement kerma value representative of the general behavior in the 1-MeV region as determined by a fit to an analytic expression having the form[8]:

$$ \kappa_{Si}^{ref}\left(E\right) = A \cdot E\left(1 - e^{-B/E}\right) \qquad (5) $$

The 1-MeV(Si)-Equivalent response function is then given by:

$$ {}^{n}\kappa_{1-MeV}(E) = {}^{n}_{type}\kappa_{displ}(E) \Big/ \kappa_{Si}^{ref}\left(1-MeV\right) \qquad (6) $$

The fifth damage metric, the NRT-based damage energy, is defined in a manner similar to that for the displacement kerma in Eq. 3, but also has a special treatment in the region near the displacement threshold energy. The displacement threshold energy, E_d, is the minimum energy imparted to the primary knock-on atom (PKA) as a result of a neutron-induced reaction that will result in a displacement of the resulting lattice atom (identical to the target lattice atom in the case of an elastic or inelastic event). The energy required to displace a lattice atom has an angle dependence due to the crystalline structure and, because small displacements can rapidly recombine, there is a large variation in the experimental determination of E_d. There is also a large variation in the calculated values[9] for E_d. Both the experimental and calculated values for E_d in crystalline silicon tend to be in the range $\in \langle 10\,eV, 30\,eV \rangle$. The Norgett-Robinson-Torrens (NRT) threshold treatment[2] defines the number of Frenkel pairs near the threshold region as:

$$ {}^{NRT}\nu_d\left(E_d, {}^{ion}T_{dam}(T_{R,j_i})\right) = $$

$$ \begin{pmatrix} 0 & 0 \le {}^{ion}T_{dam} < E_d \\ 1 & E_d \le {}^{ion}T_{dam} < 2 \cdot E_d / \beta \\ \beta \cdot {}^{ion}T_{dam} / \left(2 \cdot E_d\right) & 2 \cdot E_d / \beta \le {}^{ion}T_{dam} < \infty \end{pmatrix} \qquad (7) $$

where the damage energy for the ion is given by: ${}^{ion}T_{dam} = {}^{ion}T_{dam}^{Robinson}\left(T_{R,j_i}\right) \cdot T_{R,j_i}$

and ${}^{ion}T_{dam}^{Robinson}\left(T_{R,j_i}\right)$ is the Robinson fit to the LSS fractional partition function. A reference damage energy for an NRT-Frenkel pair can be defined as:

$$ {}^{NRT}\alpha = (2gE_d)/\beta \qquad (8) $$

where β is an atomic scattering correction and is taken to be 0.8. This reference energy can then be used to relate a damage energy to a number of displaced atoms.

When a NRT-threshold treatment is applied to the displacement kerma, the NRT-based damage energy is defined as:

$$ {}^{n}_{NRT=E_d}\kappa_{dam}(E) = \sum_{i,j_i} \sigma_{i,j_i}(E) \int_0^{\infty} dT_{R,j_i} \int_{-1}^{1} d\mu \cdot f(E,\mu,T_{R,j_i}) \cdot $$

$$ {}^{NRT}\Lambda_d[E_d, {}^{ion}T_{dam}(T_{R,j_i})] \cdot {}^{ion}T_{dam}^{Robinson}\left(T_{R,j_i}\right) \cdot T_{R,j_i} \qquad (9) $$

where

$$ {}^{NRT}\Lambda_d\left(E_d, {}^{ion}T_{dam}(T_j)\right) = $$

$$ \begin{pmatrix} 0 & 0 \le {}^{ion}T_{dam} < E_d \\ (2\cdot E_d)\,/\,(\beta g\, {}^{ion}T_{dam}) & E_d \le {}^{ion}T_{dam} < (2gE_d/\beta) \\ 1 & (2gE_d/\beta) \le {}^{ion}T_{dam} < \infty \end{pmatrix} \quad (10) $$

The Frenkel pair density, the sixth metric in Table I, has a model-dependence based on the displacement threshold treatment. For the NRT Frenkel pair density, the damage metric is given as:

$$ {}^{n}_{NRT=E_d}\kappa_{FP}(E) = \sum_{i,j_i}\sigma_{i,j_i}(E)\int_0^\infty dT_{R,j_i}\int_{-1}^{1} d\mu\cdot f(E,\mu,T_{R,j_i})\cdot $$

$$ {}^{NRT}\nu_d\left(E_d, {}^{ion}T_{dam}(T_{j_i})\right)\cdot {}^{ion}T_{dam}^{Robinson}\left(T_{R,j_i}\right)\cdot T_{R,j_i} \quad (11) $$

Since every neutron-induced interaction produces a primary recoil atom, the track density, the seventh metric in Table I, is a damage metric that is directly proportional to the total cross section.

The minority carrier lifetime, the 8th metric in Table I, is a metric based upon the Frenkel pair generation but also applies a defect efficiency function based on the recombination cross section for the minority carriers with the neutron energy-dependent defect population. There is a wide range of defects that can result from displacements in silicon, e.g. VO, V_2^-, $V_2^=$, VP. The formation rate for these defects is affected by the initial density of Frenkel pairs and the presence of dopants and contaminant atoms near the defect cluster.

The LET distribution, the 9th metric in Table I, is not a scalar damage metric, but it is described by the cumulative density function (cdf) for the recoil atom spectrum weighted by the ion energy-dependent stopping power for the initial recoil atoms. The silicon stopping power is shown in Figure 1. The ion stopping power shows a peak and then falls off with increasing ion energy. Since this LET damage metric is intended to capture the maximum charge generation within the sensitive volume of the silicon device, the proper weighting function should be the maximum stopping value for any ion energy equal to or less than that for the initial neutron-induced recoil ion energy. As seen in the figure, the maximum of the silicon stopping power occurs at about 1 MeV per nucleon, so, for fission energy neutrons, the maximum stopping power corresponds to the initial recoil energy. When neutron-induced reactions result in a heavy primary recoil particle and an alpha particle, the LET from the alpha particle should be added to that from the PKA (as well as being treated as a separate particle) in order to represent the maximum charge deposition in the device sensitive volume. Figure 2 shows the probability distribution function (pdf) for the LET distribution from a 14-MeV neutron. The cumulative LET distribution is an integral over the pdf and represents the cumulative probability for an LET being generated that exceeds a given value. Figure 3 shows the cdf for a 14-MeV neutron on silicon.

III. TREATMENT OF THE UNCERTAINTY CONTRIBUTORS

The determination of the uncertainty in the calculated damage energy requires that we look at the energy-dependent uncertainty in the various quantities in Equation 2. This energy-dependent uncertainty is best captured as a covariance function, which is equivalent to providing an energy-dependent standard deviation and a correlation matrix. The major components within the integrand of Eq. 2 are: 1) the reaction cross section and resulting recoil ion spectra; 2) the partition function that divides the recoil energy into a damage component, e.g. an ionizing component or a non-ionizing component; and 3) a threshold treatment. The following sections capture some of the primary observations on how to characterize the uncertainty due to the treatment of each of these three separate quantities. Since these components are uncorrelated, the uncertainty in the damage energy can be expressed as the sum of the component covariance matrices.

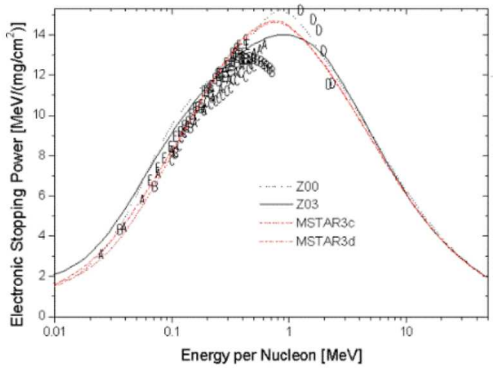

Fig. 1. Stopping power in silicon lattice

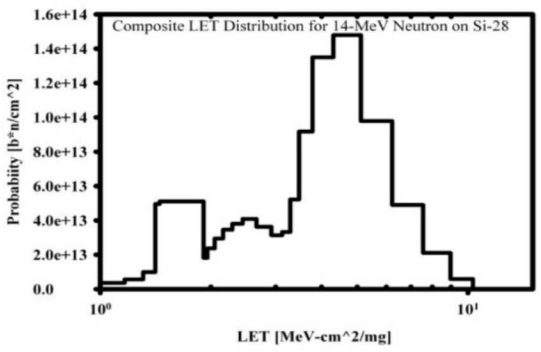

Fig. 2. pdf for silicon LET from 14-MeV neutrons

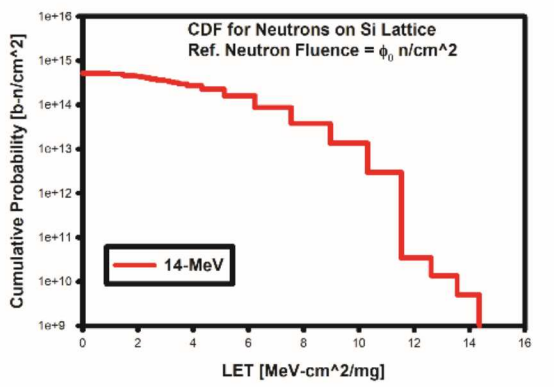

Fig. 3. cdf for Silicon LET from 14-MeV Neutron

III.A. Nuclear Data

The investigation of uncertainties in the damage energy metric starts with a consideration of the uncertainty due to the underlying nuclear data. The baseline damage energy response function is calculated for a sharp threshold Kinchin-Pease model[10] that uses the Robinson fit to the LSS damage partition function[2,3] with the NJOY-2012 code[1]. NJOY cannot only produce the total damage energy, but it can separately output the various components of the damage energy, i.e. the elastic, inelastic, and disappearance damage energy components. The residual damage component, termed as "other" here, is computed by subtracting the components from the total damage energy. For the ^{28}Si isotope, this "other" damage energy channel includes contributions from the (n,2n), (n,nα), (n,2nα), (n,np) and (n,n2α) channels. Figures 4 and 5 show a logarithmic and linear representation of the energy-dependent fractional contribution from each of these channels.

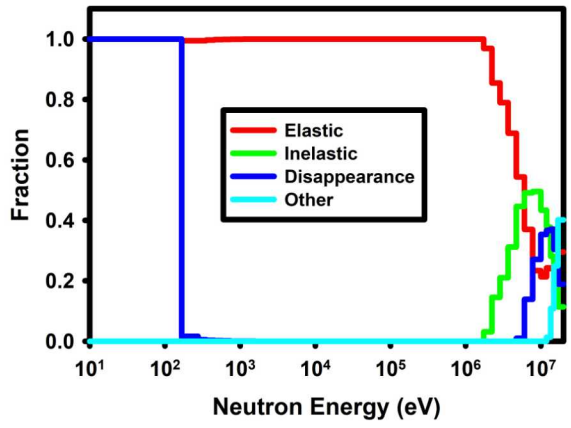

Fig. 4. Logarithmic energy view of the relative contribution of the ^{28}Si sharp threshold damage energy from reaction channels.

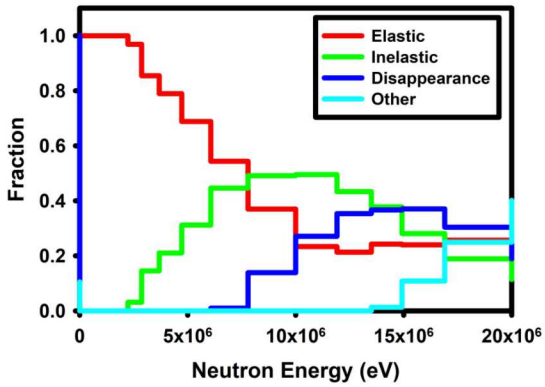

Fig. 5. Linear energy perspective of the relative contribution of high energy portion of the ^{28}Si sharp threshold damage energy from reaction channels.

The damage energy depends not just on the cross section, but also on the resulting recoil ion spectra. These recoil spectra are quite complex, varying with the incident neutron energy and the reaction channel. Figure 6 shows some representative recoil energy spectra for a 15-MeV neutron on ^{28}Si. Figure 7 shows a representative comparison of the agreement of the recoil spectrum between different evaluated nuclear data files for the (n,nα) reaction with an incident neutron energy of 20 MeV. From the broad study, the agreement is seen to be very good in the elastic channel, but there can be significant differences for some of the disappearance channels for neutron energies near the reaction threshold energy.

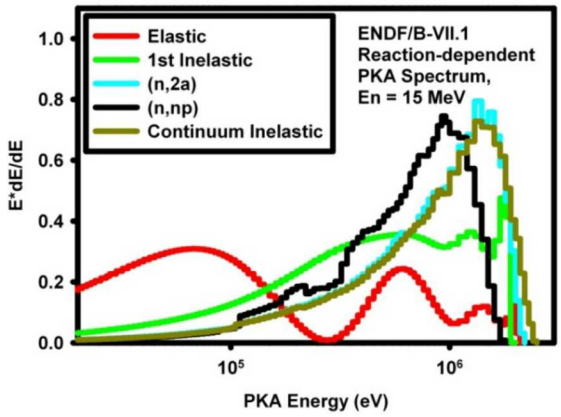

Fig. 6. Reaction-dependent recoil spectra for 15-MeV neutron

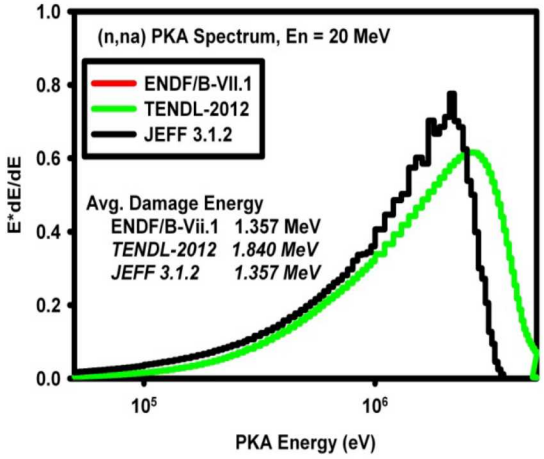

Fig. 7. Comparison of ENDF-format library dependence of the (n,nα) recoil spectra

Using a set of 300 random cross section libraries generated with the TALYS system of codes and made available as part of the TENDL-2015 release[11,12] a Total Monte Carlo (TMC) approach[13,14] was used to treat the nonlinear propagation of uncertainty through the equation that defines the damage energy. An 89-group structure was used in the NJOY-2012 code to generate a 300-element set of damage energies and then to compute the covariance matrix for the nuclear data contribution to the uncertainty for the various response functions.

Figure 8 shows the energy-dependence of the standard deviation for the various damage energy components. One immediately notes that, while the total damage energy is the sum of the various component damage energies, at high energy the uncertainty in the total damage energy is significantly smaller than the uncertainty for any of the individual components. This indicates that there is a strong correlation between the various damage energy components, a correlation that cannot be neglected in characterizing the uncertainty in the total damage energy. This study clearly shows that a sample-based, i.e. Monte Carlo, nonlinear propagation of uncertainty that fully incorporates the underlying physics-based correlations between the different reaction channels, like that provided by the TMC approach, is required for this uncertainty analysis.

Figure 9 shows the resulting standard deviations for the various damage metrics due to the nuclear data uncertainty as represented in this 300 sample TMC analysis. Figures 10 and 11 show representative correlations matrices for the ionizing kerma and the displacement kerma.

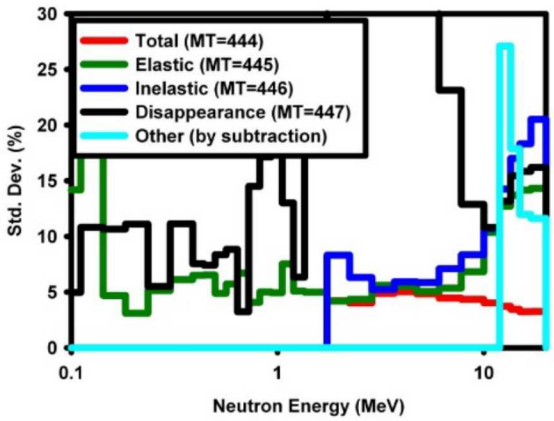

Fig. 8. Standard deviation for the ^{28}Si sharp threshold damage energy from the reaction channels.

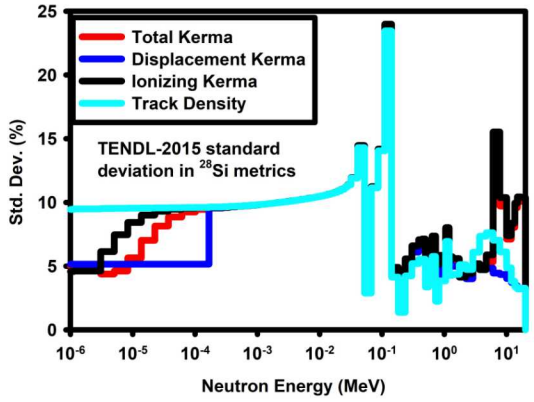

Fig. 9. Uncertainty due to nuclear data

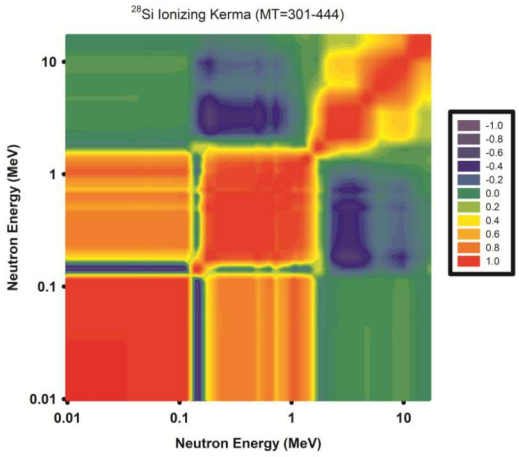

Fig. 10. ^{28}Si ionizing kerma correlation matrix due to nuclear data

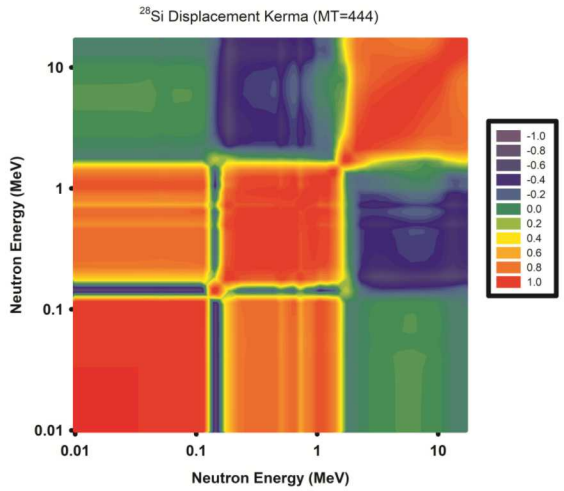

Fig. 11. ^{28}Si displacement kerma correlation matrix due to nuclear data

III.B. Partition Function

The second major source of uncertainty in Eq. 2 is from the damage partition function. This is the function ${}^{ion}T_{dam}(T_r)$ in Eq. 2 that, for the damage energy metric, converts the recoil ion energy, T_r, into a non-ionizing (displacement) component that can be correlated with the production of Frenkel pairs. The most widely used energy partition model is the Robinson fit to the Lindhard, Scharff, and Schiott (LSS) energy partition[3] that uses a Thomas-Fermi screening function over the Coulomb potential to model the elastic interactions and a non-local free uniform electron gas model for the inelastic electronic scattering. Robinson and Torrens fit[2] the LSS energy partition with an analytic representation based upon the atomic mass, A, and atomic number, Z, for the incident ion and the lattice ion. The main source of uncertainty in the partition function comes from uncertainty in the ion interaction potentials.

In order to more completely explore this sensitivity, the binary collision approximation (BCA) code, MARLOWE[15,16], was used to calculate the ion energy-dependent partition function for a range of ion interaction potentials that have been used by the ion modeling community. There are two types of potentials: those that describe the electronic interaction and those that describe the ion interaction with the lattice atoms. The former is called the electronic potential and is typically described by the LSS or ZBL potential. The latter is called the nuclear potential - even though it has nothing to do with nuclear interactions - and the MARLOWE BCA code has implemented models with the Moliere, exponential, and Lenz-Jensen potential. Figure 12 shows the set of partition functions that arose from these BCA calculations.

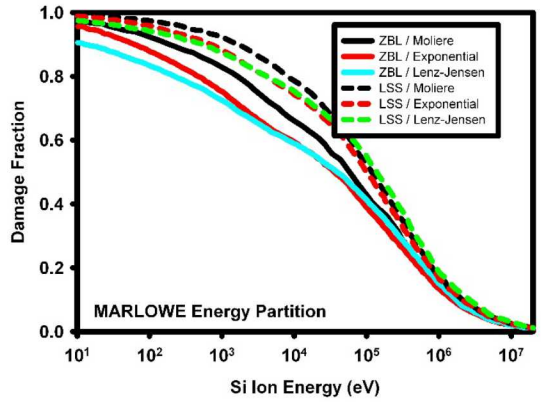

Fig. 12. Silicon displacement kerma fractions due to the different interaction potentials

After generating this range of representative partition functions, investigations showed that the cumulative Weibull distribution provided an excellent functional fit to the form of the fractional partition functions. The Weibull form had a high-quality fit to each of the individual BCA-based partition functions as well as for the composite set of data. The fits enabled the extraction of mean values and standard deviation for the 5-parameter Weibull functional form. Two constraints were used to capture observed correlations between the Weibull distribution parameters resulting in a 3-parameter fit. A Monte Carlo sampling of the fitting parameters was used to generate the covariance matrix for the ion damage energy partition function. This covariance matrix is represented by the standard deviation and correlation matrix shown in Figures 13 and 14.

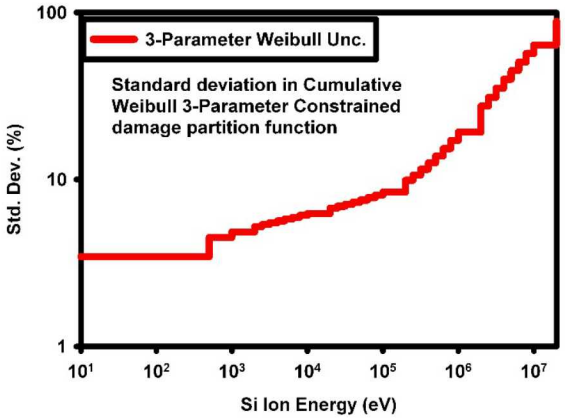

Fig. 13. Standard deviation for silicon partition function based on a Weibull distribution (5 parameter representation with 2 constraints)

When a Total Monte Carlo process is used with a set of 1000 NJOY calculations to propagate the uncertainty in the recoil ion partition function into the uncertainty contribution in the neutron energy-dependent response functions a covariance matrix is generated. Figure 15 shows the resulting neutron energy-dependent standard deviation in the ionizing and displacement kerma due to the uncertainty in the partition function. Figure 16 shows the correlation matrix for uncertainty due to the partition function in the displacement kerma. As expected from the physics of the ion energy loss and the broad energy range for recoil atoms, this correlation matrix shows a strong positive correlation for much of the neutron energy phase space.

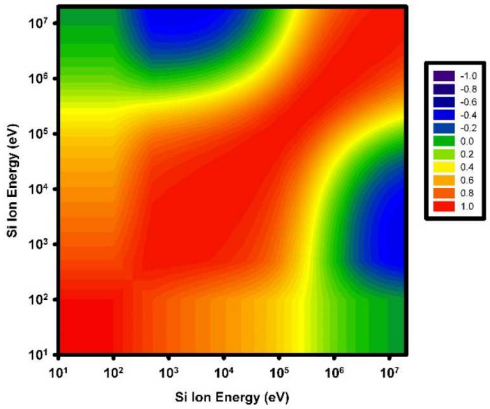

Fig. 14. Correlation matrix for silicon partition function based on a Weibull distribution (5 parameter representation with 2 constraints)

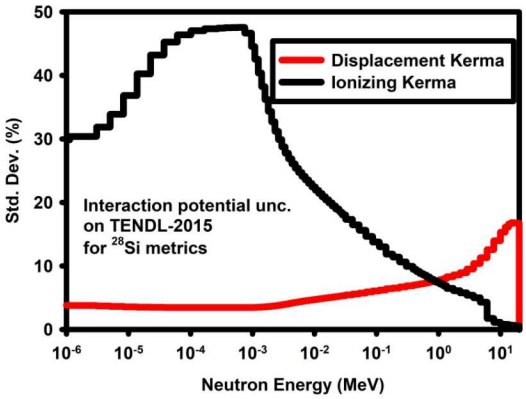

Fig. 15. ^{28}Si Uncertainty due to interaction potentials

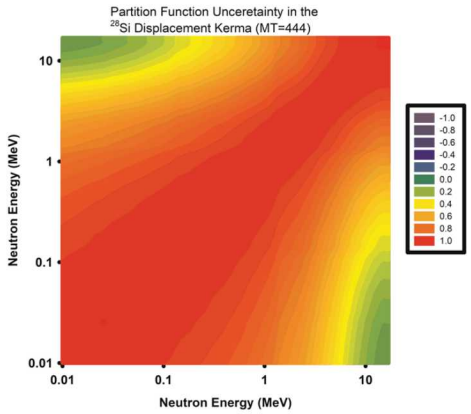

Fig. 16. ^{28}Si displacement kerma correlation matrix due to interaction potentials

III.C. Displacement Threshold Energy and Treatment

The next contribution to the uncertainty to consider is that due to the treatment of the displacement threshold region. While the displacement kerma is basically the damage energy with a zero eV lower integration bound and a zero displacement threshold energy, the damage energy for realistic cases can be strongly affected by the choice of the displacement threshold energy and by the formalism for treating the effective damage near the threshold where actual displaced lattice atoms can be generated. The nominal/recommended displacement threshold energy in silicon is 20.5 eV[17]. However, there is significant uncertainty in the value for the displacement threshold energy. For silicon, the range found in both experimental investigation and in model-based calculation is between 10 eV and 30 eV[9,17].

Figure 17 shows that the difference between the various displacement model metrics is negligible except in a narrow neutron energy range between 100 eV and 1 keV. However, the effect can be large in this region, ±50%. The difference between these damage energy metrics based on the displacement model in this neutron energy region is due to the fact that elastic scattering is the dominant reaction in this region and conservation of momentum and energy for each elastic interaction results in a maximum energy transfer to a lattice atom given by:

$$E_{recoil} = \frac{4 \cdot A \cdot E_n}{(A+1)^2} \qquad (7)$$

where E_n is the energy of the incident neutron and A is the atomic weight of the lattice atom. The case where the lattice recoil energy in silicon from elastic scattering is equal to a displacement threshold energy of 20.5 eV corresponds to an incident neutron energy of ~153 eV. For lower neutron energies, the deviations are very small since the displacement kerma is dominated by the

contributions from the (n,γ) reaction, which kinematically permits a larger recoil energy for the residual ion, so that the lower integration bound for the displacement threshold energy no longer plays an important role in the damage energy calculation.

Figure 18 shows the variation in the threshold-based damage energy, i.e. with E_d as the lower integration bound that can result from this range of possible values for the displacement threshold energy in silicon. This figure shows the percent difference relative to the nominal/recommended displacement threshold energy of 20.5 eV. The maximum deviation seen in Figure 18 between damage energies with different E_d values [relative to E_d = 20.5 eV] is seen to be about ±80% - but this is only significant over a small energy region.

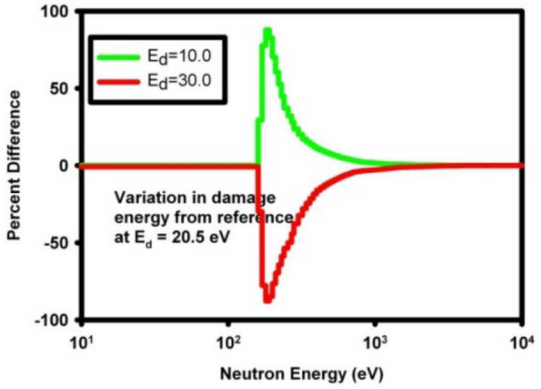

Fig. 17. Effect of varying the displacement threshold energy

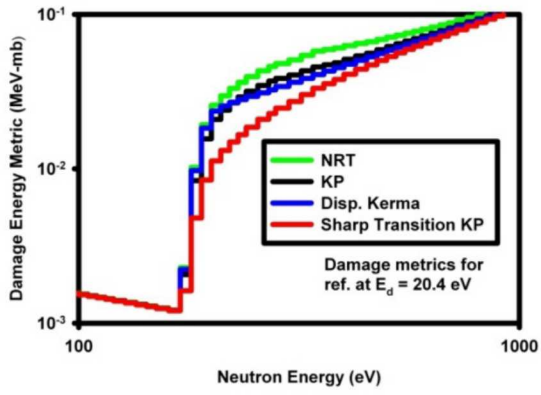

Fig. 18. Effect of different treatments of the threshold on the damage energy

In our work we have quantified the change in the damage energy when the displacement threshold energy is varied using a Total Monte Carlo approach to capture the nonlinear change in the damage energy. The energy-dependent standard deviation in the magnitude of the response is shown in Figure 19. The energy-dependent correlation matrix is shown in Figure 20.

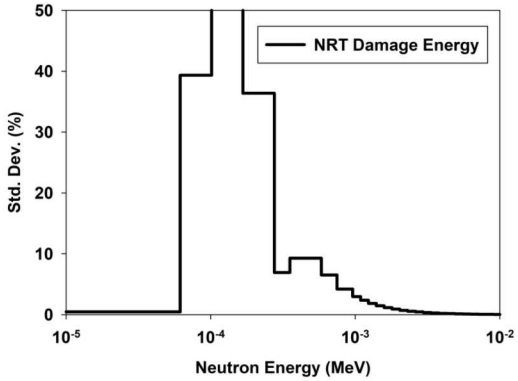

Fig. 19. ^{28}Si NRT-based damage energy uncertainty due to the threshold displacement treatment

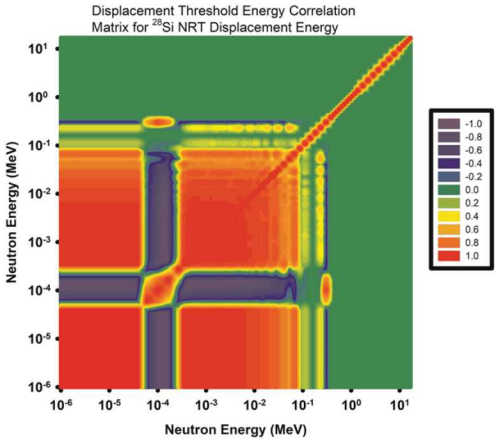

Fig. 20. ^{28}Si NRT-based damage energy correlation matrix due to the displacement treatment

III.D. Model Defect

The above sections dealt with all of the obvious contributions to the uncertainty in the damage energy. The purpose of "model defect" category is to address any uncertainty aspects that were not captured in the normal accessible parameter variation, i.e. a model attribute that did not have a user-accessible parameterized form. While we may not be able to statistically vary the "model defect" uncertainty contributions in order to characterize them, we should be able to use "subject matter expertise" to recognize the uncertainty contributions and propose, based on expert judgement, an energy-dependent term that provides for a conservative treatment of this potential uncertainty contribution.

The treatment of "model defect" varies with each response metric and is an area of active investigation and refinement. Contributions considered so far include:

1) Potential uncertainty in the underlying nuclear reaction models not captured with accessible nuclear reaction model parameter variation. An example is the expected variation in recoil energy spectra from some of the non-threshold reaction channels.
2) The may be differences in the energy-dependence of the calculated damage metric and the phenomena with which it is intended to be correlated. In particular, for silicon displacement damage, there is some experimental data that suggests that low energy neutron damage is much less than predicted with the calculated damage energy. This may be related to the fact that this damage metric was developed to correlate with the formation of primary Frenkel pair, whereas the actual change in minority carrier lifetime in silicon devices is caused by the more complex defect, i.e. divacancies and vacancy-phosphorous defects rather than the vacancy-oxygen defects that predominate from low damage energy induced point defects. The modelling of the efficiency with which Frenkel pair defects migrate and form complex defect with impurities and dopants is not captured in the currently modelled physics.
3) Some semiconductors, e.g. GaAs, indicate a thermal spike phenomenon at higher neutron energies[18], this thermal spike effect may exist in silicon at neutron energies above 20 MeV. An arc-dpa formalism[9] has a functional behaviour that could capture the recoil energy dependence of this effect if experimental evidence is gathered.

IV. RESULTS

As a sample application of the importance of the various uncertainty contributions for silicon damage metrics, consider the spectrum-averaged damage metric, as defined by Eq. 1, in the ^{252}Cf spontaneous fission benchmark neutron field. Table II shows the uncertainty contributions to the various metrics from the nuclear data (Nuc. Data.), the interaction potential (Int. Pot.), and the threshold treatment (Thresh.). Uncertainties are given in column 4 for a proper treatment using the correlation matrix as well as, in column 3, for an assumed fully correlated uncertainty. For the NRT-based damage energy, the proper treatment of the uncertainty shows that the uncertainty contribution from the interaction potential is over three times that from the nuclear data. For this same metric, there is a factor of two difference between the nuclear data uncertainty when using a proper covariance matrix as opposed to the fully correlated assumption. However, for the interaction potential uncertainty, the fully correlated and properly uncertainties are nearly identical. This is because, as seen in Figure 16, the uncertainties due to the interaction potential are nearly fully correlated.

TABLE II. Contributions from uncertainty components for the silicon damage metrics in the ^{252}Cf(sf) field.

Metric	Unc. Cont.	Uncertainty	
		Fully Correlated.	Proper Correlation
Total Kerma	Nuc. Data	6.283%	3.817%
Displ. Kerma	Nuc. Data	4.815%	2.652%
	Int. Pot.	8.964%	8.679%
Ionizing Kerma	Nuc. Data	7.299%	4.946%
	Int. Pot.	4.640%	4.487%
NRT Dam. Energy	Nuc. Data	4.815%	2.653%%
	Int. Pot.	8.964%	8.679%
	Thresh.	0.0017%	0.0009%

Table III shows the result of combining the various uncertainty contributions while distinguishing the fully and properly correlated cases shown in Table II. A proper treatment of the correlation is seen to make a factor of two difference for total kerma metric, but it does not have a large effect for the displacement or ionizing kerma metrics. This is attributed to the large uncertainty contribution from the ionization potential term and the fact that it is strongly energy correlated. Work is underway to apply the 1-MeV(Si) constraint shown in Eq. 5 to derive a proper covariance matrix for the 1-MeV response function. Since this metric is dominated by the fast neutron response, the constraint should remove most of the systematic uncertainty due to the interaction potential. This will result in the dominant uncertainty coming from the consideration of the nuclear data and, based on the uncertainty components seen in Table II, the proper correlation treatment will for the 1-MeV(Si) metric will result is a factor of three times smaller uncertainty than through use of the fully correlated model.

V. CONCLUSIONS

The above discussion has captured the recent work performed to provide a better understanding of the uncertainties in radiation damage metrics. The work reported here focused on an examination of primary radiation damage in silicon semiconductor materials that affects the change in minority carrier lifetime, and, in

particular, on properly expressing the relevant damage metric and then on quantifying the energy-dependent uncertainty of this metric in the form of a covariance matrix.

TABLE III. Importance of treating correlation in the silicon damage metrics in ^{252}Cf(sf) field.

Metric	Neutron Spectrum	Response Function	
		Fully Correlated	Proper Correlation
Total Kerma	0.374%	6.28%	3.817%
Displ. Kerma	0.162%	10.20%	9.106%
Ionizing Kerma	0.530%	8.82%	6.911%
NRT Dam. Energy	0.162%	9.95%	9.106%

REFERENCES

1. R. E. MACFARLANE, D. M. MUIR, R. M. BOICOURT and A. C. KAHLER, The NJOY Nuclear Data Processing System, Version, report LA-UR-12-27079, Los Alamos National Laboratory, Los Alamos, NM, Dec. 20, 2012.
2. M. J. NORGETT. M. T. ROBINSON, and I. M. TORRENS, "A Proposed Method of Calculating Displacement Dose Rates," *Nuclear Engineering and Design*, Vol. 33, pp. 50-54 (1975).
3. J. LINDHARD, M. SCHARFF and H. SCHIOTT, "Range Concepts and Heavy Ion Ranges," *Mat. Phys. Medd. Dan. Vld. Selsk*, Vol. 33, pp. 1-40 (1963).
4. A. AKKERMAN, and J. BARAK, "New Partition Factor Calculations for Evaluating the Damage of Low Energy Ions in Silicon," I*EEE Transactions on Nuclear Scienc*e, Vol. 53, pp. 3667 (2006).
5. J. F. ZIEGLER, J. P. BIERSACK and U. LITTMARK, The Stopping and Range of Ions in Solids, Pergamon Press, Inc., New York, 1985.
6. ASTM E722-14, Standard Practice for Characterizing Neutron Fluence Spectra in Terms of an Equivalent Monoenergetic Neutron Fluence for Radiation-Hardness Testing of Electronics, ASTM International, West Conshohocken, PA, 2014.
7. J. G. KELLY, and P. J. GRIFFIN, "Comparison of Measured Silicon Displacement Damage Ratios with ASTM E-722-87 and NJOY Calculated Damage," *Proceedings of the Seventh ASTM-EURATOM Symposium on Reactor Dosimetry*, Strasbourg, France, Aug. 1990, p. 711, Kluwer Academic Publishers, Boston (1992).
8. A. L. NAMESON, E. A. WOLICKI, and G. C. MESSENGER, "Average Silicon Neutron Displacement Kerma Factor at 1 MeV", *IEEE Transactions on Nuclear Science, NS-29,* No. 1, pp. 1018-1020 (1972).
9. Primary radiation damage in materials - Review of Current Understanding and Proposed New Standard Displacement Damage Model to Incorporate In-Cascade Defect Production Efficiency and Mixing Effects, OECD/NEA Working Party on Multiscale Modelling of Fuels and Structural materials for Nuclear Systems, Expert Group on Primary Damage, NEA/NSC/DOC(2015)9 (2015).
10. G. H. KINCHIN and R. S. PEASE, "The Displacement of Atoms in Solids by Radiation", *Reports on Progress in Physics*, Vol. 18 (1955).
11. A. J. KONING, D. ROCHMAN, et al., TENDL-2015: TALYS-based evaluated nuclear data library", https://tendl.web.psi.ch/tendl_2015/tendl2015
12. A. J. KONING, and D. ROCHMAN, Modern Nuclear Data Evaluation with the TALYS Code System, *Nuclear Data Sheets*, 113, pp. 2841 (2012).
13. D. ROCHMAN, A. KONIG, S. C. VAN SER MARCH, A. HOGENBIRK and D. VAN VEEN, "Nuclear Data Uncertainty Propagation: Total Monte Carlo vs. Covariances," *Journal of Korean Physics*, **59**, 1236-1241 (2011).
14. D. ROCHMAN, A. KONIG, S.C. VAN DER MARCK, A. HOGENBIRK and D. VAN VEEN, "Nuclear Data Uncertainty Propagation: Total Monte Carlo vs. Covariances," *Journal of Korean Physics*, Vol. 59, pp. 1236-1241 (2011).
15. M. T. ROBINSON and O. M. TORRENS, "Computer Simulation of Atomic-Displacement Cascades in Solids in the Binary-Collision Approximation," *Physical Review B*, **9**, 5008 (1974).
16. M. T. ROBINSON, MARLOWE Binary Collision Cascade Simulation Program, Version 15b, A Guide for Users (2002).
17. P. J. GRIFFIN, Relationship between Metrics used to Represent Displacement Damage in Materials, report SAND-2014-3341, Sandia National Laboratories, Albuquerque, NM, (2014).
18. P. J. GRIFFIN, J. G. KELLY, T. F. LUERA, A. L. BARRY, and M. S. LAZO, "Neutron Damage Equivalence in GaAs," *IEEE Transactions on Nuclear Science*, NS-38, No. 6 (1991).